J Am Oil Chem Soc (2010) 87:715–730
DOI 10.1007/s11746-010-1553-6

ORIGINAL PAPER

Properties and Stability of Solid Lipid Particle Dispersions Based on Canola Stearin and Poloxamer 188

C. Celeste Trujillo · Amanda J. Wright

Received: 28 May 2009 / Revised: 1 February 2010 / Accepted: 9 February 2010 / Published online: 14 March 2010

Abstract Solid lipid particles (SLP) are one strategy for encapsulating lipophilic molecules, including for controlled release and enhanced bioavailability applications. SLP based on fully hydrogenated canola stearin (CaSt, 5, 10, 20, and 30 wt%) and the non-ionic surfactant Poloxamer 188 (P188, 0.0, 0.5, 1.0, 2.5, 5.0 and 10.0 wt%) were produced by high pressure melt homogenization using a microfluidizer. Spherical particles in the region of 140 nm were formed, depending on compostion and processing parameters. Surfactant concentration and pressure had a significant influence on particle diameter ($P < 0.05$), although number of homogenization cycles did not ($P > 0.05$). A maximum surfactant surface load of approximately 4 mg m^{-2} was observed and, at or above 2.5% P188, excess surfactant was present in the continuous phase after production. P188 had the effect of decreasing particle size and facilitating transitions from the α to the β polymorph ($P < 0.05$) both through surface nucleation and size reduction effects. A stability study of the 10% CaSt SLP with 0.0, 1.0, or 5.0% P188 revealed particle growth for the 0.0 and 1.0% P188 SLP, especially at 20 versus 4 °C, but no changes in the 5.0% P188 SLP, which were exclusively in the β form, at both temperatures for up to 240 days.

Keywords Solid lipid particles · Canola stearin · Poloxamer 188 · Particle diameter · Polymorphism · Surfactant surface load · Melting · Crystallization · Stability

C. C. Trujillo · A. J. Wright (✉)
Department of Human Health and Nutritional Sciences, University of Guelph, Guelph, ON N1G 2W1, Canada
e-mail: ajwright@uoguelph.ca

Introduction

Solid lipid particles (SLP) have been proposed as an attractive delivery strategy for lipophilic compounds [1–3]. In particular, molecules with no or limited water solubility present unique challenges because of their aggregation tendencies in aqueous environments and limited bioavailability. SLP may enhance the encapsulation potential in these cases and possess the advantages that they can be produced with non-toxic ingredients without the need for solvents and large-scale production is feasible. Also, due to their solid nature, there is the potential to improve loading and for controlled release of encapsulated compounds, in comparison to emulsions. Despite the intense interest in SLP, there are challenges to overcome to capitalize on their potential for widespread use. These include the tendency for supercooling, particle growth, unexpected sample gelation and polymorphic transitions. Furthermore, the crystalline structure of SLP, while offering advantages, may ultimately limit the encapsulation potential of SLP for some compounds [4], particularly when appropriate crystal structures are not produced.

SLP shape and structure are critical in determining the efficiency of loading and release of encapsulated compounds. For example, spherically shaped isometric SLP with minimal order in the crystalline state tend to have higher loading capacities and controlled encapsulated compound release potential as compared to thin platelets with highly ordered and dense structures [5]. Dispersed and bulk fats also exhibit pronounced differences in terms of their crystallization and melting, with implications for SLP functionality [6]. Lipid polymorphism is a key consideration since it influences SLP physicochemical properties, including the capacity to incorporate molecules [7, 8]. SLP containing α crystals may undergo polymorphic transitions

during storage or thermal processing, with an accompanying rearrangement of the TAG molecules and possible expulsion of molecules encapsulated within the core [6, 9]. Furthermore, polymorphic transitions from the α to β form in SLP have been previously related to SLP destabilization, sometimes evidenced by gelation of an SLP dispersion and a change from a spherical to a platelet shape [10, 11].

Interactions between the crystallizing TAG and surfactants play a key role in defining SLP behavior [12] and significant differences have been reported for SLP of differing compositions and based on exposure to different conditions, indicating a high degree of system specificity. A better understanding of the relationships between SLP production, physicochemical properties and stability is required in order to capitalize on SLP encapsulation potential. This study was undertaken to determine the effects of composition and processing on properties of SLP based on fully hydrogenated canola stearin (CaSt) and Poloxamer 188 (P188). Poloxamers are non-ionic, water-soluble, tri-block copolymer steric stabilizers consisting of polyethylene oxide (PEO) and polypropylene (PPO) blocks as PEO-PPO-PEO. They are well characterized and have demonstrated potential for SLP production, including for nano-sized particles (i.e. solid lipid nanoparticles, SLN) [13] and are commonly used in industrial, pharmaceutical, natural health product and cosmetic applications, although they are not food-grade. Poloxamers exhibit minimum toxicities, may enable controlled release and targeted delivery applications and are stable at high temperatures. Also, SLP containing only P188 are generally not optimally stable, making it possible to study the underlying mechanisms related to SLP instability. SLP containing CaSt and P188 were produced by high pressure melt homogenization using a microfluidizer and the effects on particle size, morphology, melting, polymorphism, surfactant surface concentration and stability were determined.

Materials and Methods

Fully hydrogenated canola stearin (CaSt) was generously provided by Bunge Canada (Toronto, ON, Canada). The material had a melting point of 68 °C, a fatty acid composition of 84.6% stearic acid, 8.6% palmitic acid, 2.8% oleic acid, and 1.7% linoleic acid, and a triacylglycerol composition of 0.7% PPP, 1.2% PPS, 5.1% SOS, 9.4% SSP and 79% SSS, where P, S, and O are palmitic, stearic and oleic acids, respectively [14]. The concentration of mono- and diacylglycerols in the CaSt was less than 0.1 wt% and no free fatty acids were detected. The steric, non-ionic emulsifier poloxamer 188 (i.e. P188, Lutrol® F 68, polyoxyethylene–polyoxypropylene polymer with a hydrophilic–lipophilic balance of 29 at 25 °C) was generously provided by BASF (Florham Park, NJ, USA).

SLP Production by High Pressure Homogenization (HPH)

CaSt (5, 10, 20 or 30 wt%) was heated at 95 °C for 30 min after melting in order to erase crystal memory. The surfactant (0.0, 0.5, 1.0, 2.5, 5.0 or 10.0 wt% of the aqueous phase) was dissolved in Milli Q water and also heated to 95 °C before being homogenized with the CaSt at 10,000 rpm for 30 s using a handheld mixer (Ika T18 Basic). This hot, pre-emulsion was subsequently passed one, three, five or ten times through a M110-EH Microfluidizer Processor (Microfluidics Corporation, Newton, MA, USA) maintained at ~80 °C using an immersion bath and operated at the desired pressure (34.5, 69, 103, 138 or 174 MPa). The resulting emulsions were stored in 20 mL vials at 22 ± 2 °C with no exposure to light or air in order for the lipids to crystallize, forming the SLP. Newtonian cooling was observed, with samples reaching 42, 30 and 22 °C by 8, 30 and 170 min, respectively. Samples were analyzed, in the form of SLP dispersions, 24 h after production. At least three separate batches of each sample were prepared and three replicate measurements of each sample were performed.

Particle Diameter by Laser Diffraction (LD)

The volume weighted mean diameter ($D_{4,3}$) was determined by (LD) using a Mastersizer 2000 with a Hydro 200 SM sample handling unit (Malvern Instruments, EUA) and accompanying software and using refractive indices of 1.455 and 1.33, respectively, for CaSt and water. Where indicated, the emulsifying activity index (EAI, m^2 surface area/g emulsifier) was calculated from the surface weighted mean diameter ($D_{3,2}$) and the total emulsifier concentration.

Melting Behavior by Differential Scanning Calorimetry (DSC)

A DuPont model 2910 differential scanning calorimeter (TA Instrument, Mississauga, ON, Canada) was used to study the bulk fat and SLP melting behavior. Between 10–12 mg of the SLP samples and 6–8 mg of the bulk CaSt were accurately weighed into aluminum pans and hermetically sealed. Samples were heated from 20 to 85 °C at 5 °C per min. Attempts were made to study the crystallization behavior of the SLP immediately after homogenization. Unfortunately, the samples invariably crystallized during loading into the DSC pans. Therefore, recrystallization runs were carried out after melting by holding the melted samples in the DSC at 85 °C for 15 min and then cooling at

5 °C per min to −10 °C. Recognizing that melting might have led to changes in particle size, samples were analyzed by LD and then melted at approximately 5 °C per min to 85 °C, held for 15 min and then cooled to 22 °C and left for 24 h before reanalysis by LD. Values of $D_{4,3}$ before and after the described temperature cycling were not significantly different (i.e. 6.3 vs. 6.5 μm, 0.71 vs. 0.79 μm, 0.34 vs. 0.35 μm, 0.13 vs. 0.13 μm, and 0.13 vs. 0.13 μm for the 0.0, 1.0, 2.5, 5.0, and 10.0% P188 SLP, respectively, $P > 0.05$). Therefore, the effects of particle size on the behavior observed during the DSC recrystallization experiments should approximate the initial SLP crystallization behavior. Peak melting and recrystallization temperatures (T_m and T_{rc}) and melting enthalpies (ΔH_m) were calculated using the TA Universal Analysis software provided.

Polymorphism by Powder X-Ray Diffraction (XRD)

A Rigaku Multiplex powder X-ray diffractometer (Rigaku Corporation, Japan) was used to determine the polymorphism of the SLP samples, using Bragg's Law and following background subtraction with MID's Jade 6.5 software. Scans were performed from 1 to 30° at 0.5° per min at a controlled temperature of 20 °C. Assignment of the polymorphic form was based on spacings of 4.1, 4.2 and 3.8, and 4.6 Å for the alpha (α), beta prime (β') and beta (β) polymorphs, respectively [15].

Microstructural Investigations by Polarized Light and Cryo-Scanning Electron Microscopy (PLM and Cryo-SEM)

For imaging by polarized light microscopy (PLM), one drop of the SLP sample was pipetted onto a glass slide and carefully covered with a glass cover slip. Images were acquired using a Leica DMRXA2 upright light microscope (Leica Microsystems, Toronto, Canada) equipped with a digital monochrome camera (QImaging Retiga® 1300, Vancouver, Canada). Images were taken using 10 and 40× objective lenses (Leica, Germany) and captured using Openlab 5.5.0 (Improvision, Canada).

A Hitachi S-570 scanning electron microcopy (SEM) (Hitachi High Technologies, Tokyo, Japan) was used to investigate the size and morphology of the SLP. Samples, prepared, in duplicate, were injected into stainless steel rivets mounted on a copper holder for the EMI Tech K1250x (Ashford, Kent, UK) cryo-preparation unit. The holder was plunged into a liquid nitrogen slush (at −207 °C) under vacuum and removed from the chamber through argon to prevent frost formation on the surface. Frozen samples were then fractured and sublimated for 90 min at −80 °C and coated with 30 nm of gold (EMI tech K1250x Sputter Coater, Ashford, Kent, UK). Images were captured digitally (PCI Quartz; Quartz Imaging Corp. Vancouver, BC, Canada).

Rheological Properties by Small Deformation Testing

The 10% CaSt SLP containing 0.0, 1.0 and 5.0% P188 were analyzed after production by small deformation rheology using a AR 2000 controlled stress rheometer (TA Instruments, New Castle, DE, USA) equipped with an acrylic cone-place geometry (plate diameter 60 mm, cone angle 2°). Continuous flow experiments with shear rates from 0.5–300–0.5 s^{-1} and oscillatory stress sweeps from 0–10 Pa at a frequency of 1 Hz were conducted.

Sample Preparation and Storage for Stability Study

To study SLP stability over time, samples were prepared, as described above, with three passes through the microfluidizer at 69 MPa and containing 10% CaSt with 0.0, 1.0, and 5.0% P188. 0.01% sodium azide was added to inhibit microbial growth. After crystallization for 24 h at 22 ± 2 °C, samples were analyzed in triplicate for particle diameter, melting behavior and polymorphism. They were also placed at 4 and 20 °C and analyzed, in triplicate, after 7, 14, 30, 60, 90, 180 and 240 days storage for particle diameter, melting behavior and polymorphism.

Determination of P188 Surface Load (Γ_s)

The P188 surface load (Γ_s) was calculated according to $\Gamma_s = C_a D_{3,2}/6\Phi$, where C_a is the mass of emulsifier adsorbed to the surface per unit volume of sample, $D_{3,2}$ is the volume-surface mean diameter, and Φ is the dispersed phase volume fraction (i.e. 10% CaSt) [16]. To determine the amount of emulsifier adsorbed onto the surface, the concentration of P188 remaining in the aqueous phase was obtained by centrifuging the SLP after production (which included 24 h crystallization at 22 °C) at 130,000 *g* and 22 °C for 12 h and filtering the aqueous phase (0.1 μm). P188 concentration was determined using a colorimetric assay, as previously described [17]. Briefly, 200 μl of aqueous phase, or diluted aqueous phase, were combined in a 2-mL microcentrifuge tube with 100 μl dye reagent (consisting of 3 g cobalt (II) nitrate, 20 g ammonium thiocyanate and 100 mL water), 200 μl ethyl acetate and 80 μl absolute ethanol. The samples were mixed thoroughly and then centrifuged at 10,400*g* for 1 min. The two upper layers were aspirated and the pellet and tube walls washed several times with 200 μl ethyl acetate until the wash solvent was colorless, at which point the pellet was dissolved in 2 mL acetone and the absorbance at 624 nm determined using a Hewlett Packard 8451A diode array spectrophotometer. P188 concentrations were calculated

based on a standard curve prepared from solutions (0.0–0.5%) of P188 in Milli Q water. The detection threshold limit of the assay was 0.02% P188 and $r^2 = 0.98$.

Statistical Analysis

Overall effects of CaSt and P188 concentrations and processing parameters (pressure and number of passes) were studied using Statistical Analysis Software 9.1.3. Where main effects were observed, multiple comparison testing was done using Tukey's test. GraphPad Prism (Version 4.0) was used to perform *t* tests, one- and two-way ANOVA and $P < 0.05$ was considered the level of significance.

Results and Discussion

Effect of Composition and Processing on SLP Diameter

Particle size has a critical influence on the potential uses and stability of SLP. SLP size depends on the nature of the lipid matrix, the type and amount of the emulsifying agent used, as well as the processing conditions, including temperature and the shear forces generated [18]. Table 1 shows the volume weighted mean diameter ($D_{4,3}$) of SLP prepared with variable CaSt (5, 10, 20, and 30%) and P188 (0.5, 1.0, 2.5, and 5.0%) concentrations and processed at 69, 103, 134, or 172 MPa with one homogenization cycle (i.e. one pass through the microfluidizer). Samples for which gelation was observed and particle size could not be determined are indicated as 'gelled'. Figure 1 shows the effect of homogenization energy density (34.5, 69, 103, 134 and 172 MJ m^{-3}) on the 24 h $D_{4,3}$ and emulsifying activity index (EAI) in subsequent studies conducted with a wider range of P188 concentration (0.0 and 10.0%), pressures (34.5 MPa) and multiple homogenization cycles (3, 5 and 10 passes) for the samples which showed the highest stability and reproducibility in Table 1, i.e. for the particles prepared using 10% CaSt.

Effects of lipid and surfactant concentrations as well as homogenization pressure were observed ($P < 0.05$). However, there was no overall effect of varying the number of passes through the microfluidizer ($P > 0.05$). At the lowest lipid contents studied (i.e. 5 and 10% CaSt) the dispersions were more stable (i.e. smaller particles and less tendency for aggregation) and particle size was more reproducible (i.e. lower standard deviation between replicates). This was especially the case when a low CaSt content was combined with a relatively high P188 concentration. The SLP formed ranged in diameter from 0.14 to 32.32 μm. The smallest particles were formed with 5% CaSt ($P < 0.05$), followed by those produced with 10, 20 and 30% lipid. This is partly related to sample viscosity during production [18]. At high CaSt concentrations, larger particles result because the higher particle numbers increase the probability of droplet or particle contact and subsequent aggregation [19].

As expected, surfactant concentration had a clear effect on SLP diameter. The relative small size of the SLP in the absence of P188 was somewhat surprising. It is postulated that the high degree of crystallinity achieved very early after homogenization (CaSt has a melting temperature of ~68 °C) minimized coalescence and partial coalescence of the crystallizing droplets. The possibility that the CaSt contained surface active partial acylglycerols or free fatty acids was considered. However, the concentration of mono- and diacylglycerols was less than 0.1% and the free fatty acid content negligible.

$D_{4,3}$ decreased significantly for each CaSt concentration studied with increasing P188 concentration ($P < 0.05$). For example, SLP produced with 5% CaSt (69 MPa, 3 passes) were 1.40 versus 0.15 μm with 0.5 versus 5.0% P188, respectively ($P < 0.05$). The effect of P188 was even more obvious at higher lipid contents. With 20 and 30% CaSt, samples containing only 0.5% P188 gelled immediately after production. However, with 1.0 and 5.0% P188, the 20% CaSt SLP (69 MPa, 3 passes) were 20.63 versus 0.39 μm. Also, the 20% CaSt SLP with 1.0% P188 gelled when processed at 172 MPa, but not at the lower pressures. As discussed below, this is explained by the higher energy inputs creating smaller droplets, but insufficient emulsifier present to stabilize the created interface.

The effect of P188 concentration is highlighted by Fig. 2 which shows the particle distributions for the 10% CaSt SLP (69 MPa, 3 passes) with variable P188 concentration. In the absence of P188, a bimodal distribution with peaks located around 0.9 and 9.0 μm was observed. Smaller particles were evident with increasing P188, although 10.0% surfactant was required to achieve a monomodal distribution, as even the 5.0% P188 samples possessed a small shoulder around 0.6 μm.

Figure 1 shows that varying the energy density and number of homogenization cycles had little impact on the emulsifying activity index (EAI) within each P188 concentration. A decrease in EAI did tend to be observed at 172 MJ m^{-3} for the 0.5% P188 samples. This was likely related to the presence of insufficient surfactant molecules to stabilize the newly created interface at the highest pressure. With 1 (e), 3 (f), 5 (g), or 10 (h) passes through the microfluidizer, EAI decreased with increasing total surfactant. The highest EAI values were observed with only 0.5% P188, suggesting an inefficiency of additional surfactant molecules to create or stabilize more surface area. However, 0.5% P188 was not sufficient to create nano-sized particles (Table 1). Also, the EAI calculation assumes that all the emulsifier present is located at the

Table 1 Effect of P188 concentration (0.5, 1.0, 2.5 and 5.0%) and processing pressure (69, 103, 134, 172 MPa) on 24 h particle size ($D_{4,3}$, μm) of canola stearin-poloxamer 188 solid lipid particles prepared with 5, 10, 20 and 30% CaSt after three passes through the microfluidizer

	P188 Concentration (%)			
	0.5	1.0	2.5	5.0
5% CaSt (MPa)				
69	$1.40 \pm 0.34^{a,1}$	$0.42 \pm 0.03^{b,1}$	$0.20 \pm 0.01^{b,1}$	$0.15 \pm 0.01^{b,1}$
103	$1.12 \pm 0.25^{a,1}$	$0.53 \pm 0.06^{a,b,1}$	$0.26 \pm 0.02^{b,1}$	$0.19 \pm 0.02^{b,1}$
134	$1.55 \pm 0.35^{a,1}$	$1.03 \pm 0.15^{a,b,1}$	$0.44 \pm 0.05^{b,c,1}$	$0.14 \pm 0.00^{c,1,3}$
172	$2.52 \pm 0.50^{a,2}$	$0.85 \pm 0.10^{b,3}$	$0.37 \pm 0.04^{b,c,3}$	$0.13 \pm 0.00^{c,3}$
10% CaSt (MPa)				
69	$1.57 \pm 0.28^{a,1}$	$1.26 \pm 0.29^{a,1,3}$	$0.42 \pm 0.42^{a,1,3}$	$0.20 \pm 0.02^{a,1,3}$
103	$3.32 \pm 0.64^{a,1}$	$0.41 \pm 0.04^{a,1,3}$	$0.67 \pm 0.67^{a,1,3}$	$0.32 \pm 0.03^{a,1,3}$
134	$3.95 \pm 0.68^{a,1}$	$1.33 \pm 0.23^{a,1}$	$0.61 \pm 0.61^{a,1}$	$0.21 \pm 0.02^{a,1}$
172	$32.32 \pm 10.94^{a,2}$	$2.99 \pm 0.55^{b,3}$	$0.78 \pm 0.78^{b,3}$	$0.29 \pm 0.03^{b,3}$
20% CaSt (MPa)				
69	Gelled*	$20.63 \pm 2.30^{a,1}$	$1.05 \pm 0.15^{b,1}$	$0.29 \pm 0.03^{b,1}$
103	Gelled*	$9.98 \pm 1.21^{a,2}$	$0.58 \pm 0.07^{b,1}$	$0.25 \pm 0.02^{b,1}$
134	Gelled*	$22.24 \pm 1.93^{a,1}$	$5.38 \pm 1.89^{b,1,3}$	$0.40 \pm 0.06^{c,1}$
172	Gelled*	Gelled*	$3.77 \pm 0.44^{a,3}$	$0.75 \pm 0.08^{b,1}$
30% CaSt (MPa)				
69	Gelled*	Gelled*	Gelled*	0.36 ± 0.04^{1}
103	Gelled*	Gelled*	Gelled*	3.87 ± 1.71^{1}
134	Gelled*	Gelled*	Gelled*	2.57 ± 1.10^{1}
172	Gelled*	Gelled*	Gelled*	Gelled*

Values represent means ± SEM, $n = 3$

Homogenization pressures correspond to energy densities of 69, 103, 134, and 172 MJ m^{-3}

Different superscript letters (a, b, c) within each row indicates significant difference between values ($P < 0.05$)

Different superscript numbers (1, 2, 3) within each column indicates significant difference between values within each CaSt concentration (i.e. within 5, 10, 20 or 30%) ($P < 0.05$)

* Samples could not be analyzed because they gelled immediately after production

interface and, as discussed below for Table 3, this was not the case at all P188 concentrations.

Increasing the number of passes through a homogenizer is a common strategy to achieve particle size reductions [20]. However, overall, there was no effect of number of cycles on particle diameter in Fig. 1. Within each pressure or energy density, smaller particles tended to be formed with three versus only one pass, but additional passes did not generally achieve further size reductions. Similar results were reported for SLP produced by valve homogenization with 10% trilaurin (Dynasan 112) and 5% P188 in that the most efficient homogenization was observed with three cycles and at 50 MPa [13]. It is commonly observed that beyond a certain number of passes, droplet size cannot be further decreased [21]. In the absence of surfactant, smaller particle sizes were also not observed with multiple homogenization cycles.

Table 1 and Fig. 1 show that, while $D_{4,3}$ tended to increase with homogenization pressure (or energy density), the effect was highly dependent on P188 concentration. In some cases, increases in particle diameter were observed at higher pressures. For example, values of $D_{4,3}$ were higher with 1.0% P188 as the pressure was increased, with three, five, or ten passes (see Fig. 1). Similar trends were observed for the 20% CaSt SLP, comparing the values of $D_{4,3}$ with 103 versus 134 MPa (see Table 1). Smaller droplets are produced at higher pressures and more surfactant is needed. Also, the rate of poloxamer adsorption to droplet surfaces is reportedly slow, owing to their relatively high molecular weights (8,400 g mol^{-1} for P188) [22, 23]. While high pressures lead to greater droplet disruption, if the surfactant is not able to adsorb to the created interfaces quickly enough, coalescence will occur, leading to larger emulsion droplets [24] and ultimately larger SLP. Such 'over-processing' can result at high energy inputs during very efficient homogenization operations, particularly microfluidization [21] and depends on factors such as the nature and concentration of the lipid and surfactant, the

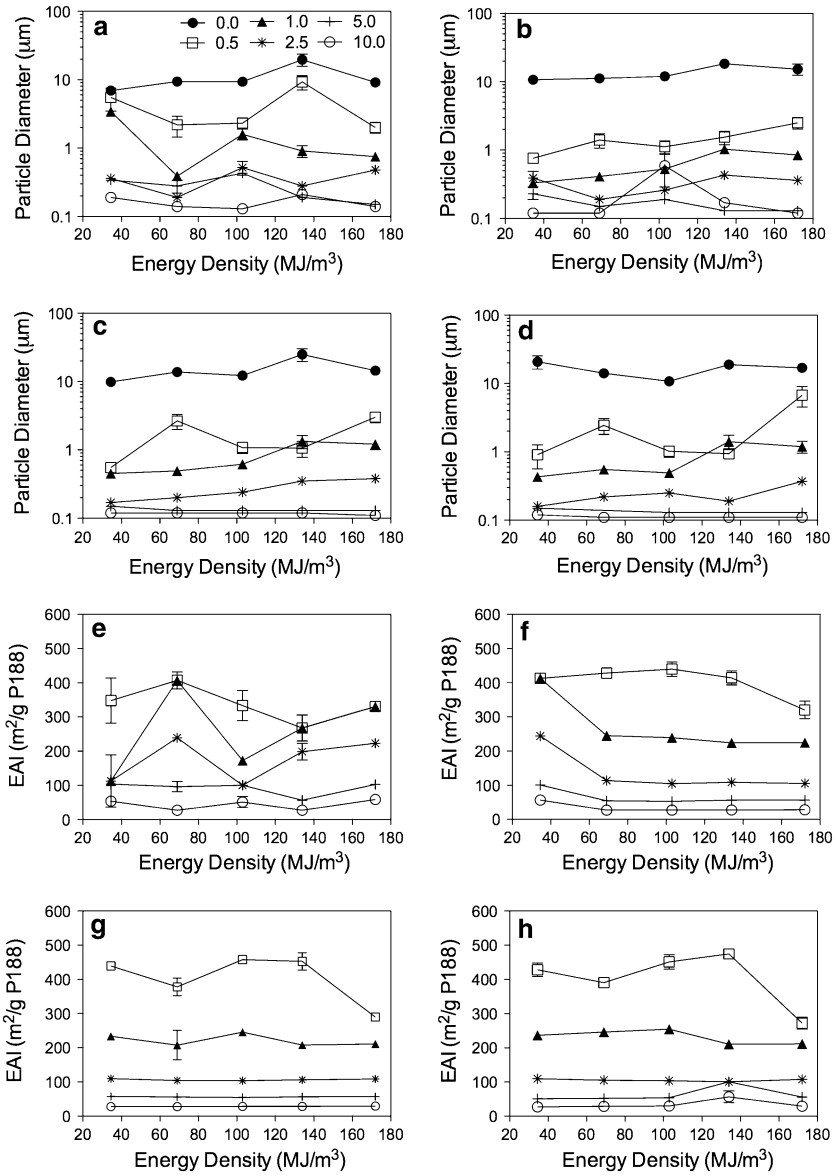

Fig. 1 Effect of homogenization energy density (34.5, 69, 103, 134 and 172 MJ m^{-3}, equivalent to homogenization pressures of 34.5, 69, 103, 134 and 172 MPa) on 24 h particle size ($D_{4,3}$, μm; **a**–**d**) and emulsifying activity index (EAI, m^2 g^{-1}; **e**–**h**) for 5% canola stearin-poloxamer 188 solid lipid particles prepared with P188 (0, 0.5, 1.0, 2.5, 5.0 and 10.0%) with 1 (**a**, **e**), 3 (**b**, **f**), 5 (**c**, **g**), or 10 (**d**, **h**) homogenization cycles and crystallized at 22 °C for 24 h

total energy input and homogenizer design [20, 21]. While the nature of poloxamer may have contributed to 'over-processing' at the highest pressures, P188 was very effective at the lower and more industrially relevant pressures.

The 5 and 10% CaSt SLP ranged in diameter from 120 to 200 nm, depending on P188 concentration and processing pressure. Therefore, production of solid lipid nanoparticles (SLN) is possible with this system. Similar diameters have been reported for tristearin-rich SLP stabilized with a mixture of P188 and phospholipids (i.e. 158 nm mean particle diameter by photon correlation spectroscopy [25]). Also, SLP produced by HPH and composed of 10% tripalmitin with 3.6% P188 (of the aqueous phase) were 187 nm [8], while 10% trilaurin-SLP with 5% P188 (of the aqueous phase) and also produced by HPH were 168 nm [13]. These comparisons indicate that SLP within the same size range can be produced by microfluidization as by high pressure valve homogenization. Furthermore, nanometer-sized SLP were produced at 69 MPa and with no more than three cycles, conditions which are similar to reports for valve homogenizers [1, 6, 8, 19, 26–31]. These conditions do differ, however, from recent reports of SLP production by microfluidization at much higher pressures with tripalmitin and Tween 20, i.e. 10 cycles at 900 MPa [11, 32].

SLP Melting and Polymorphic Behavior by DSC and XRD

Representative thermograms for bulk CaSt and the 10% CaSt SLP with varying surfactant concentration are shown

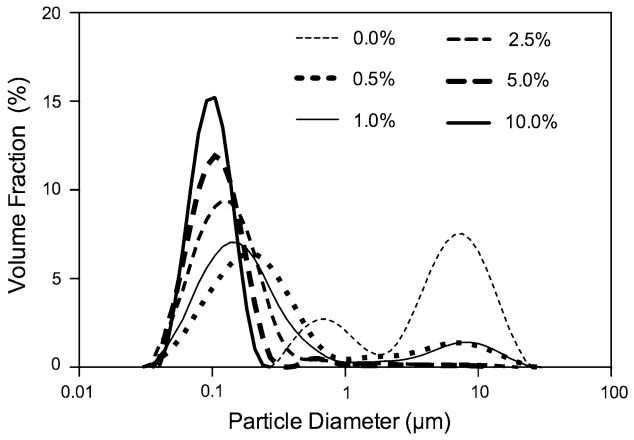

Fig. 2 Particle size distributions by laser diffraction showing the effect of P188 concentration (0.0, 0.5, 1.0, 2.5, 5.0 and 10.0%) for the 10% CaSt SLP processed at 69 MPa, with 3 homogenization cycles and crystallized at 22 °C for 24 h

in Fig. 3. The corresponding peak melting temperatures (T_m) and enthalpies (ΔH_m) are reported in Table 2.

Melting peaks corresponding to the α (~57.5 °C), β' (~64.5 °C) and β (~69.9 °C) polymorphs were observed for the bulk CaSt. This is in close agreement with reports that the α, β', and β polymorphs of tristearin melt at 56, 66, and 73 °C, respectively [33]. Compared to the bulk state, T_m for the dispersed samples was significantly lower ($P < 0.05$). For example, T_m of the α, β' and β polymorphs were 57.5, 64.5 and 69.9 °C, respectively, for the bulk CaSt versus 52.9, 60.7 and 67.9 °C, respectively, for the SLP without surfactant. Lipid dispersions typically melt around 3–5° lower than their respective bulk samples because of the decrease in particle size and as expected according to the Gibbs–Thomson equation [6, 26, 27, 34]. Emulsifier type and concentration and production method can also account for differences in melting behavior between lipid dispersions and the corresponding bulk fat [8, 35, 36].

According to Table 2, the α polymorph was present in each of the 0.0, 0.5, 1.0, 2.5 and 5.0% P188 SLP samples 24 h after production, but not with 10.0% P188. T_m for the α polymorph was the same regardless of surfactant concentration ($P > 0.05$) and despite differences in particle diameter. Other reports, however, have noted a T_m depression with decreasing particle size [6, 8, 9, 26–28]. Lower values of $\Delta H_{m\alpha}$ were observed for the 2.5 and 5.0% P188 SLP, compared with the 0.5 and 1.0% P188 SLP, indicating the presence of less α with increasing emulsifier molecules. In fact, the $\Delta H_{m\alpha}$ for the 5.0% P188 SLP was only 0.1 J g^{-1} and no α peak was detected in the 10% P188 SLP.

The β' polymorph was only observed in the bulk CaSt and 0.0% P188 SLP. Its absence in the P188-containing samples is consistent with the hypothesis that P188 facilitates transitions to the β form. Also, as little as 0.5% P188 changed the SLP polymorphism. This suggests the surfactant interacts directly with TAG molecules at the interface, initiating polymorphic transitions there where TAG molecules have higher mobilities compared with those in the core of a crystal lattice [37]. Smaller particles were also observed with increasing P188 concentration. In smaller particles the number of TAG molecules per particle able to interact with interfacial surfactant molecules is also relatively higher [12]. In some cases, interactions between TAG and surfactant molecules can delay polymorphic changes [12]. However, in this study, increases in P188 concentration were clearly associated with promotion of the α to β transition. Similar findings have been reported for other colloidal dispersions versus bulk fats, including SLP which contain hydrophilic surfactants and particularly in formulations with non-ionic stabilizers such as poloxamer [6, 37].

The influence of P188 on the CaSt SLP polymorphism is at least partly related to the direct effects on TAG crystallization. However, the effects may also be indirect because of decreases in particle size. For example, smaller particles do have a greater tendency for supercooling because the critical number of nuclei molecules required is less likely to be present as droplet size decreases [1]. According to Table 2, decreases in particle diameter and acceleration to the β polymorph were associated with increasing P188 concentration. Reports differ in terms of the relationship between polymorphism and droplet size. Because smaller droplets have higher surface curvatures, their ability to adopt more stable configurations can be restricted [12]. However, smaller particles may also experience accelerated transitions because of overall higher surface areas and the fact that molecules at the interface have higher mobility which enables the conformational changes associated with a polymorphic transition [37]. Apparent discrepancies in SLP polymorphic behavior are not surprising given the strong dependency on lipid matrix, surfactant, cooling rates, temperature and particle size. To better understand the behavior observed in this study, the relationship between P188 surface load, specifically, and particle size and polymorphism is discussed below.

Isothermal powder XRD was used to confirm the polymorph assignments by DSC. Table 2 shows that, according to XRD, the bulk and dispersed CaSt samples without P188 (i.e. bulk CaSt and the 0.0% P188 SLP) contained only the α polymorph. This is consistent with the DSC results and suggests that dispersing the fat did not affect the TAG crystallization polymorphism. Furthermore, it indicates that the β' and β peaks in the bulk CaSt and 0.0% P188 SLP thermograms were the result of transitions induced by heating the samples during analysis. The DSC and XRD

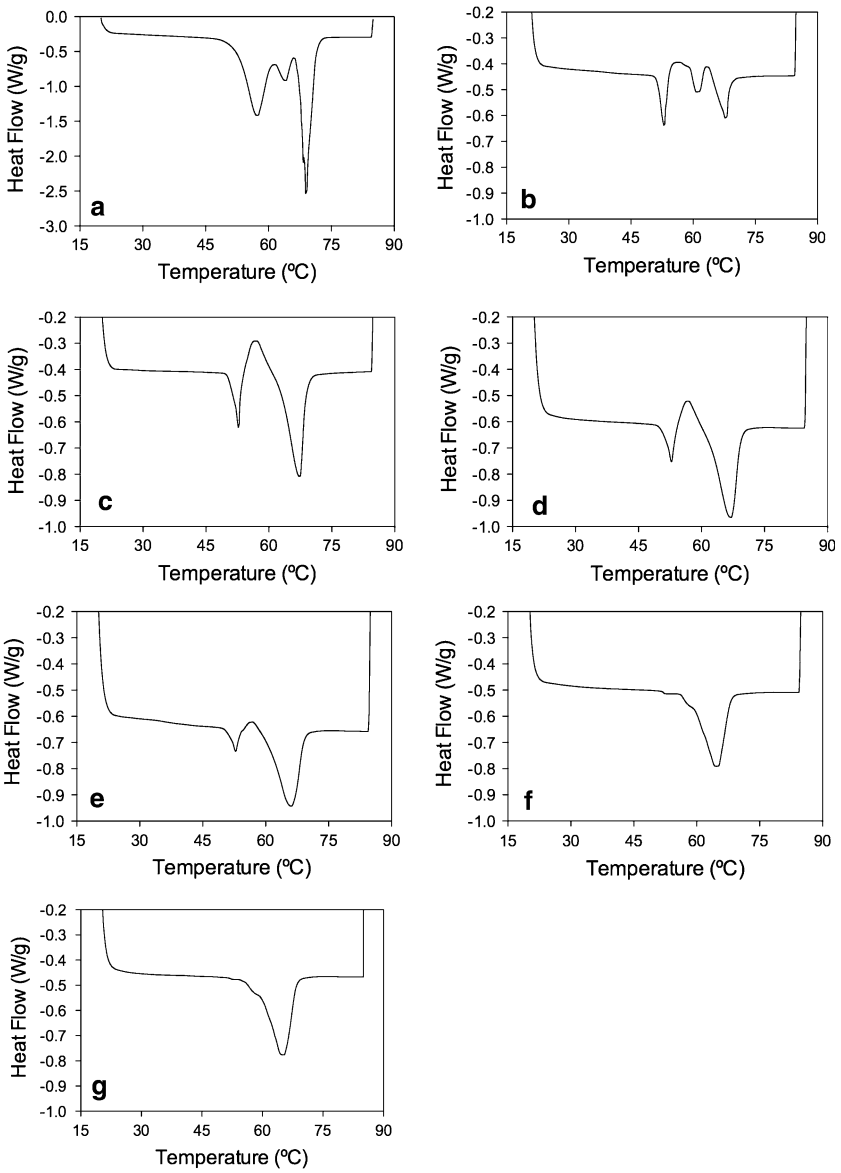

Fig. 3 Differential scanning calorimetry thermograms of bulk CaSt (**a**) and SLP containing 10% CaSt with 0.0% (**b**), 0.5% (**c**), 1.0% (**d**), 2.5% (**e**), 5.0% (**f**), or 10.0% (**g**) P188 with 3 homogenization cycles at 69 MPa and crystallized at 22 °C for 24 h

results for the 0.5% P188 SLP indicate the presence of the α and β polymorphs, both confirming the presence of β and indicating the sample was transitioning from the α to the β form at the time of measurement. According to the DSC and XRD results, P188 facilitated the α to β transition. With 5.0% P188, only the β polymorph was observed by XRD (by DSC a very small peak in the α region was observed, i.e. $\Delta H_m = 0.1$ J g^{-1}). Only the β polymorph was detected in the SLP containing 10.0% P188 by both DSC and XRD.

Supercooling is a common occurrence in SLP, particularly, but not exclusively, in those containing short chain TAG [38]. Crystallization indices are sometimes calculated from melting enthalpies in an attempt to quantify the proportion of SLP lipids which are crystallized [34]. However, this can be problematic when multiple polymorphs are present. According to Table 2, the melting enthalpy for the dispersed system containing 10% CaSt and no surfactant (i.e. 0.0% P188 SLP) was roughly 10% that of the bulk (i.e. 4.4/38.9). This indicates a high degree of crystallinity of the lipid present. For the SLP containing P188, both the α and β or just the β polymorphs were observed, as were continual decreases in the enthalpy values for both the α and β melting peaks. This suggests the presence of relatively less crystallized lipid with increasing P188 concentration, possibly related to a greater degree of supercooling with decreased particle diameter. However, this must be considered in light of the observation that P188 accelerated formation of the β phase, as discussed below.

Table 2 Peak melting temperatures (T_m, °C) and enthalpies (ΔH_m, J g^{-1}) by differential scanning calorimetry, polymorphs identified by X-ray diffractometry and particle diameter ($D_{4,3}$) by laser diffraction for bulk CaSt and SLP containing 10% CaSt with 0.0, 0.5, 1.0, 2.0, 5.0 or 10.0% P188, after 24 h crystallization at 22 °C following three passes through the microfluidizer at 69 MPa

	Differential scanning calorimetry results						Polymorph assignment by XRD	Particle size $D_{4,3}$ (μm)
	Alpha (α)		Beta-prime (β′)		Beta (β)			
	T_m	ΔH_m	T_m	ΔH_m	T_m	ΔH_m		
Bulk CaSt	57.5 ± 0.6[a]	38.9 ± 4.0[a]	64.5 ± 0.5[a]	4.8 ± 0.52[a]	69.9 ± 0.3[a]	58.0 ± 4.2[a]	α	–
0.0% P188 SLP	52.9 ± 0.0[b]	4.4 ± 0.4[b,c,d]	60.7 ± 0.1[b]	3.0 ± 0.4[b]	67.9 ± 0.3[b]	6.2 ± 1.3[b]	α	8.656 ± 0.763[a]
0.5% P188 SLP	52.7 ± 0.1[b]	7.6 ± 0.6[b]	–	–	67.1 ± 0.1[c,d]	28.0 ± 1.6[c,d]	α, β	1.574 ± 0.062[b]
1.0% P188 SLP	52.8 ± 0.2[b]	5.8 ± 0.3[b,c]	–	–	66.7 ± 0.2[d]	26.7 ± 1.2[d]	α, β	1.256 ± 0.128[b]
2.5% P188 SLP	52.6 ± 0.2[b]	2.2 ± 0.6[c,d]	–	–	65.7 ± 0.3[e]	20.2 ± 1.4[e]	α, β	0.417 ± 0.001[c]
5.0% P188 SLP	52.5 ± 0.1[b]	0.1 ± 0.0[d]	–	–	64.5 ± 0.1[f,g]	19.4 ± 0.8[e]	β	0.203 ± 0.053[d]
10.0% P188 SLP	–	–	–	–	64.5 ± 0.1[g]	20.6 ± 0.4[e]	β	0.128 ± 0.001[d]

Values represent means ± SEM, $n = 3$

Assignment of the polymorphic form was based on spacings of 4.1 Å for α, 4.2 and 3.8 Å for β′, and 4.6 Å for β [15]

Recrystallization peak temperatures (°C) for the bulk CaSt (49.7 ± 0.3), 0.0% P188 SLP (49.6 ± 0.0), 1.0% P188 SLP (49.5 ± 0.2 and 33.2 ± 0.1), 2.5% P188 SLP (49.6 and 31.8 ± 0.2), 5.0% P188 SLP (30.1 ± 0.1), and 10.0% P188 SLP (29.0 ± 0.1) were observed and obtained by holding melting DSC samples at 85 °C for 15 min and cooling to −10 °C at 5 °C per min

Different superscript letters within each column indicate significant difference between values ($P < 0.05$)

Relationship Between SLP Diameter and Polymorphism as a Function of P188 Concentration and Surface Load

Tables 1 and 2 highlight the fact that an increase in P188 was associated with a decrease in particle diameter ($P < 0.05$). P188 concentration and decreases in particle diameter were also correlated with a higher proportion of β (Table 2). The 0.0% P188 SLP contained a large population of particles in the range of 9 μm (Fig. 1) and only the α polymorph was observed (Table 2), whereas the 10.0% P188 SLP had only particles in the range of 120 nm and the β polymorph. Between 1.0 and 10.0% P188, bimodal size distributions and both α and β polymorphs were observed.

According to Table 2, T_m for β reached a plateau after 2.5% P188, i.e. in the same region as submicron sized particles were formed. In addition, a decrease in $T_{m\beta}$ was observed with an increase in P188 and associated decreases in $D_{4,3}$ (i.e. $T_{m\beta}$ was 67.9 and 64.5 °C for the 0.0 and 5.0% P188 SLP, respectively, $P < 0.05$). Also, larger particles and more broad size distributions were observed with only 0.5 and 1.0% P188 compared with the higher P188 concentrations (Fig. 2). Although not observed here, samples with wide size distributions can exhibit melting peak broadening because each size grouping has a unique melting event [4].

DSC recrystallization experiments were carried out for the SLP after each melting run. The following peak recrystallization temperatures (T_{rc}) were observed for the bulk CaSt (49.7 ± 0.3 °C), 0.0% P188 SLP (49.6 ± 0.0 °C), 1.0% P188 SLP (49.5 ± 0.2 and 33.2 ± 0.1 °C), 2.5% P188 SLP (49.6 and 31.8 ± 0.2 °C), 5.0% P188 SLP (30.1 ± 0.1 °C), and 10.0% P188 SLP (29.0 ± 0.1 °C). Only α crystallization was identified in the bulk CaSt and SLP without P188. In contrast, crystallization of both α and β was observed with 0.5, 1.0 and 2.5% P188 and only β crystallization was observed for the 5.0 and 10.0% P188 SLP. Therefore, the polymorphs formed during the recrystallization experiments were the same as present in the samples prior to melting, with the exception of the 5.0% P188 SLP where a tiny α melting event was present (Fig. 3), but no $T_{rc\alpha}$ was observed.

Comparing the T_{rc} values, no depression in α nucleation temperature was observed when CaSt was dispersed ($P > 0.05$). Emulsified lipids often crystallize at lower temperatures than bulk fat because of a decreased likelihood of heterogeneous nuclei [36] and there are reports of decreased crystallization temperature with decreasing particle size [26]. These trends may not have been observed here because of CaSt's high melting point and very rapid crystallization of the α phase. In the case of β, the T_{rc} decreased steadily from 33.2–31.8–30.1–29.0 °C for the 1.0, 2.5, 5.0 and 10.0% P188 SLP, respectively ($P < 0.05$), suggesting a greater degree of supercooling with P188 concentration and reduction in particle diameter. The P188 surface load in the 2.5, 5.0 and 10.0% P188 SLP was the same (Table 3, see discussion below, $P > 0.05$), so differences should not be related to differences in P188 surface concentration and any associated direct effects on crystallization. Also, according to Table 2, the β phase was more prominent with increasing P188. In order to better understand the time course of α and β formation, XRD

Table 3 Surface weighted mean droplet diameter ($D_{3,2}$, μm), concentration of surfactant remaining in the aqueous phase after production (%P188) and P188 surface load (mg m^{-2}) for SLP containing 10% CaSt with 0.0, 0.5, 1.0, 2.0, 5.0 or 10.0% P188, after 24 h crystallization at 22 °C following three passes through the microfluidizer at 69 MPa

SLP sample	Surface weighted mean diameter ($D_{3,2}$, μm)	Specific surface area (m^2 g^{-1})	P188 concentration remaining in aqueous phase (%)	P188 surface load (mg m^{-2})
0.0% P188	3.28 ± 0.568^{a}	1.82 ± 0.34^{a}	0.00 ± 0.00^{a}	0.0 ± 0.0^{a}
0.5% P188	0.191 ± 0.017^{b}	31.15 ± 2.70^{b}	0.00 ± 0.00^{a}	1.6 ± 0.0^{ab}
1.0% P188	0.156 ± 0.031^{b}	38.72 ± 5.84^{b}	0.03 ± 0.00^{a}	2.1 ± 0.6^{ab}
2.5% P188	0.119 ± 0.003^{b}	49.44 ± 1.34^{c}	0.47 ± 0.07^{a}	4.0 ± 0.1^{b}
5.0% P188	0.116 ± 0.007^{b}	50.81 ± 3.18^{c}	2.80 ± 0.43^{b}	4.1 ± 0.8^{b}
10.0% P188	0.114 ± 0.000^{b}	51.67 ± 0.15^{c}	8.03 ± 0.69^{c}	3.7 ± 1.3^{b}

Values represent means ± SD, $n = 3$

Different superscript letters within each column indicate significant difference between values ($P < 0.05$)

scans of the 5.0 and 10.0% P188 SLP were performed starting from 1 and up to 57 h after homogenization, as shown in Fig. 4.

For the 5.0% P188 SLP at 1 h, Fig. 4a shows a main peak at 4.14 Å, a less prominent peak around 4.59 Å and strong liquid phase scattering. Therefore, both of the α and β polymorphs are present. The α peak at 4.14 Å is gone by 7 h and the prominence of the β phase scattering continues to increase with time, as does the long spacing peak at 15.27 Å. Long spacings in the range of ~45 Å (corresponding to the 003 peak observed at 15.27 Å), indicative of a 2L lamellar crystalline structure, were observed for all SLP samples. This is consistent with reports of a long spacing at 44.98 Å for tristearin with a double chain-length packing [39]. According to Fig 4b, a very weak α peak and a very prominent β peak were observed after 1 h crystallization of the 10.0% P188 SLP. There was no evidence of α remaining by 2 h, indicating that higher concentrations of P188 accelerate β formation.

While the above DSC and XRD results indicate the important role of P188 in terms of inducing β formation, they do not distinguish between a direct effect of P188 concentration on β nucleation versus an indirect effect through reductions in particle size. Therefore, samples of the 0.0% P188 SLP were homogenized prior to the addition of hot P188 solutions to achieve final concentrations of 0.5, 1.0, 5.0 and 10.0% surfactant and then held at 85 °C for 24 h, with regular mixing, prior to crystallization at 22 °C for 24 h and subsequent analysis by LD and DSC. Particles in the range of 10 μm were observed for each sample (i.e. 10.4, 9.8, 9.4, 10.8, and 11.3 μ for the 0.0, 0.5, 1.0, 5.0 and 10.0% P188 samples, respectively, $P > 0.05$) because of challenges in evenly distributing the surfactant. However, only the α polymorph was observed for the 0.0% P188 SLP, while every sample with P188, contained both α and β (data not shown). Therefore, P188 clearly induces β formation, even in relatively large particles. There were no trends in terms of the relative prominence of the α versus β polymorphs as a function of P188 concentration in this experiment, suggesting P188 does not only act directly. It is possible that decreased particle size accelerates β formation, although Table 2 and Fig. 4 clearly show an acceleration to β in the 10.0 versus 5.0% P188 SLP where small particles with similar $D_{4,3}$ values were observed (0.203 ± 0.053 versus 0.128 ± 0.001 μm, respectively, $P > 0.05$).

To determine if particle size or surfactant interfacial concentration were responsible for the acceleration to β, P188 surface loads in the 0.0–10.0% P188 SLP were determined. Table 3 shows the surface weighted mean droplet diameter ($D_{3,2}$), specific surface area, concentration of surfactant remaining in the aqueous phase after SLP production and the P188 surface load for the 0, 0.5, 1.0, 2.0, 5.0 and 10.0% P188 SLP.

The P188 surface loads were in the range of a few mg m^{-2}, consistent with previous reports [16]. The results also reveal that excess P188 is present in the aqueous phase above approximately 2% surfactant. Excess surfactant can be required to form versus to stabilize an emulsion [40]. A trend towards higher P188 surface load with increasing total P188 was observed, although the values for the 0.5–10.0% P188 SLP were not significantly different ($P > 0.05$) and leveled off by 2.5% P188. The similar surface load values indicate that approximately the same amount of emulsifier is required to cover the same amount of interface, suggesting the particles are similarly shaped. According to Tables 2 and 3, $D_{3,2}$ and $D_{4,3}$ depended significantly on total P188 concentration ($P < 0.05$), although where differences were observed differed between the two parameters. Values of $D_{4,3}$ ranged more widely and were generally higher than for values of $D_{3,2}$. For example, $D_{3,2}$ in the range of 200 nm were observed for the 0.5% P188 SLP, whereas values of $D_{4,3}$ in the range of 200 nm were not observed until with 5.0% P188. Differences between the surface and volume weighted mean diameters can occur

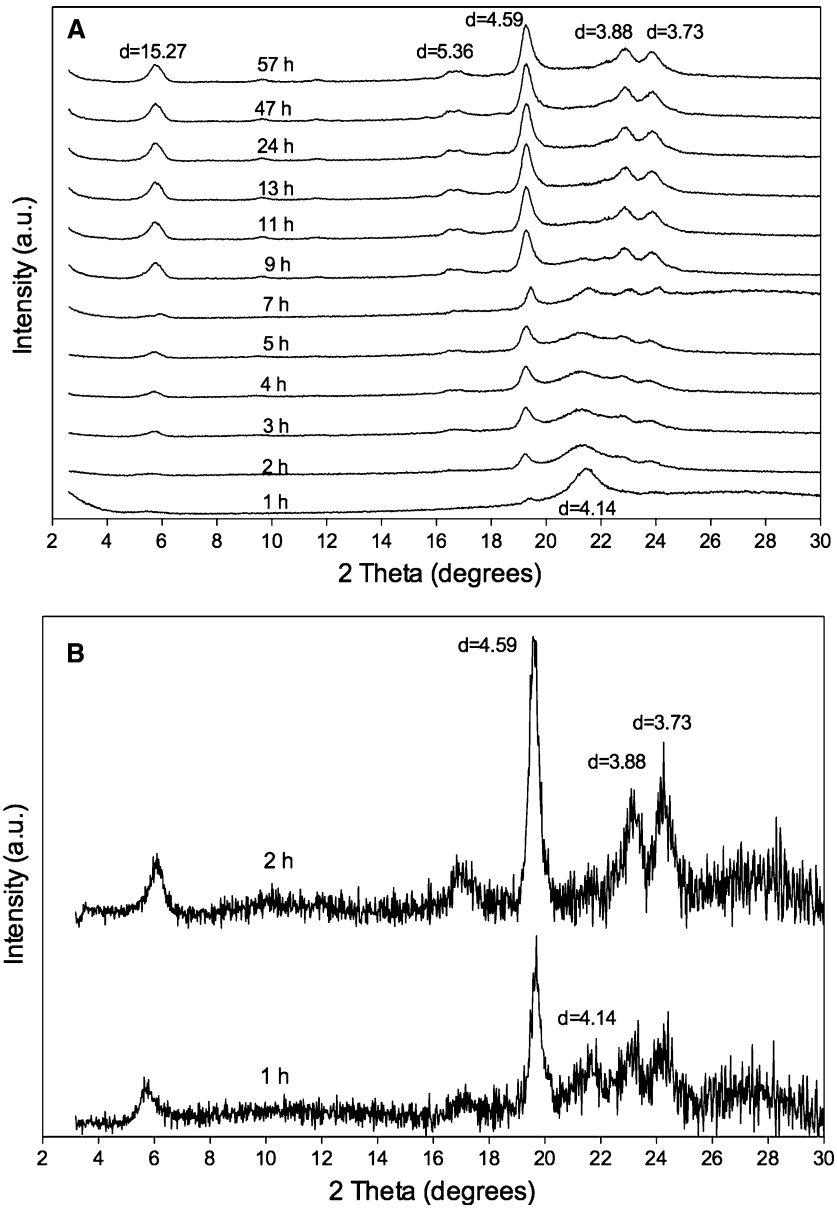

Fig. 4 Powder X-ray diffractograms for 10% CaSt SLP containing 5.0% P188 (**a**) and 10.0% P188 (**b**) produced with three homogenization cycles at 69 MPa and crystallized at 22 °C for up to 57 h

in cases of broad or multimodal particle size distributions [16], as were observed at the lowest surfactant concentrations, in particular (Fig. 2).

Combined, the results indicate that P188 induced formation of the β polymorph. Also, above $\sim$2% total P188, excess surfactant was present in the aqueous phase, with surface load reaching a maximum of approximately 4 mg m^{-2} in the 2.5% P188 SLP. Therefore, the accelerated α to β transitions associated with increases in total P188 above 2.5% P188 cannot be attributed to differences in surfactant surface load. The acceleration to β in the 2.5 versus 5.0 versus 10.0% P188 SLP must be related to differences in particle size. Thus, in this system, P188 facilitates the α to β transition through both direct and indirect effects.

SLP Rheology by Small Deformation Testing

Rheological analysis of the 0.0, 1.0, and 5.0% P188 SLP revealed very different behaviors for the SLP in the absence and presence of P188. Based on continuous flow experiments, the 1.0 and 5.0% P188 SLP were found to be non-Newtonian pseudoplastic fluids, without yield stresses. They demonstrated thixotropic behavior and had apparent viscosities of $6.0 \pm 0.1 \times 10^{-3}$ Pa s and $9.2 \pm 2.1 \times 10^{-3}$ Pa s, respectively ($P < 0.05$). Differences in the concentration of P188 remaining in the aqueous phase (i.e. 0.03 ± 0.00 vs. 2.8 ± 0.43% for the 1 and 5% P188 SLP, respectively) might account for the differences in apparent viscosity. In contrast, the 0.0% P188 SLP demonstrated viscoelastic behavior based on oscillatory testing.

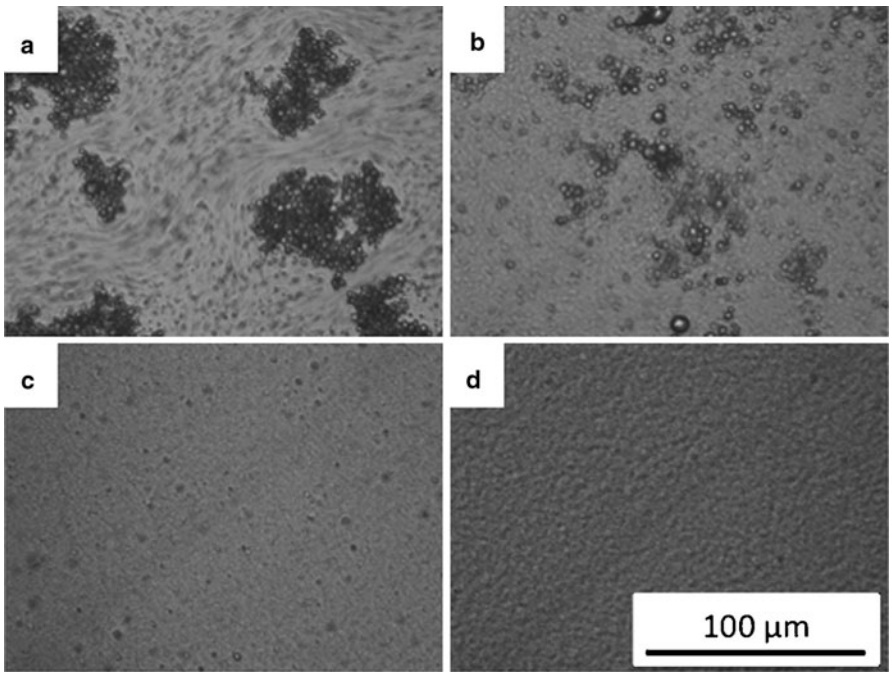

Fig. 5 Polarized light micrographs of SLP containing 10% CaSt and 0.0% (**a**), 1.0% (**b**), 5.0% (**c**) and 10.0% (**d**) P188 processed with three passes through the microfluidizer at 69 MPa followed by crystallization at 22 °C for 24 h (40× magnification)

A complex modulus of 755.52 ± 617.33 Pa was observed, although the results were highly variable, possibly because of shear-induced aggregation during the analysis.

SLP Microstructure by PLM and Cryo-SEM

Polarized light micrographs (PLM) for the 10% CaSt SLP processed at 69 MPa with three passes and containing varying amounts of P188 (0.0, 0.5, 1.0, 2.5, 5.0 and 10.0%) are shown in Fig. 5. Samples were visualized both in situ and after dilution (1:4 vol:vol dilution with Milli Q water, images not shown). In the absence of P188, clumped 0.0% P188 SLP clusters ranging in diameter from roughly 11 to 46 µm were observed (Fig. 5a). With increasing P188 concentration, less clumping was observed, although size estimates for individual SLP still could not be achieved. According to Fig. 5, generally rounded particles were observed, regardless of the presence or concentration of P188. This is in accordance with other studies reporting a spherical shape for SLP [41, 42].

Cryo-SEM was also used to image the 0.0, 1.0, 5.0, and 10.0% P188 SLP after crystallization at 22 °C for 24 h. Representative images are shown in Fig. 6. In the absence of P188 (Fig. 6a), large clumped sphere-like particles connected by thin strands, appearing to consist of tiny clumped particles, were observed. The highly aggregated nature was expected based on the absence of surfactant. By LD, particles in the 0.0% P188 SLP samples ranged from roughly 0.3 to 23.0 µm. The smallest particles discernable in Fig. 6a are around 0.2 µm.

With 1.0% P188 (Fig. 6b) rounded, aggregated SLP were again observed. The clumps appear to be smaller than for the 0.0% P188 SLP, expected in accordance with the trends by LD and given the presence of surfactant which facilitates the creation of smaller particles during homogenization and stabilizes the system during storage [40]. Also, the strands present in these samples appear to be longer than for the 0% P188 SLP, possibly due to interfacial P188 forming bridges between particles.

Large differences were seen for the 5.0 and 10.0% P188 SLP (Fig. 6c, d). A clear network of smooth strands was obvious and appeared to coat the particles. With 10.0% P188, discrete fat particles could not be seen and the strands were thicker. Such a network is consistent with reports for P188 alone and reports that P188 forms porous structures on lipophilic surfaces [43]. P188 solutions were also prepared and imaged exactly as for the SLP samples in Fig. 6, revealing long thin strands similar to Fig. 6d (data not shown). Therefore, the apparent networks in the SLP samples are related to excess surfactant in the continuous phase, especially in the 5.0 and 10.0% P188 SLP. To explore the influence of a P188 network on stabilization of the concentrated samples, the 10.0% P188 SLP was diluted after production to contain 0.5, 1.0 or 5.0% surfactant. After equilibration at 22 °C for 24 h, values of $D_{4,3}$ for the non-diluted 10.0% P188 SLP and for the 5.0, 1.0 and 0.5% P188 diluted samples were determined and did not differ significantly (i.e. ~0.13 µm, $P > 0.05$). This supports the conclusion that the apparent networks in the SEM images are not permanent and that a P188 network is not required

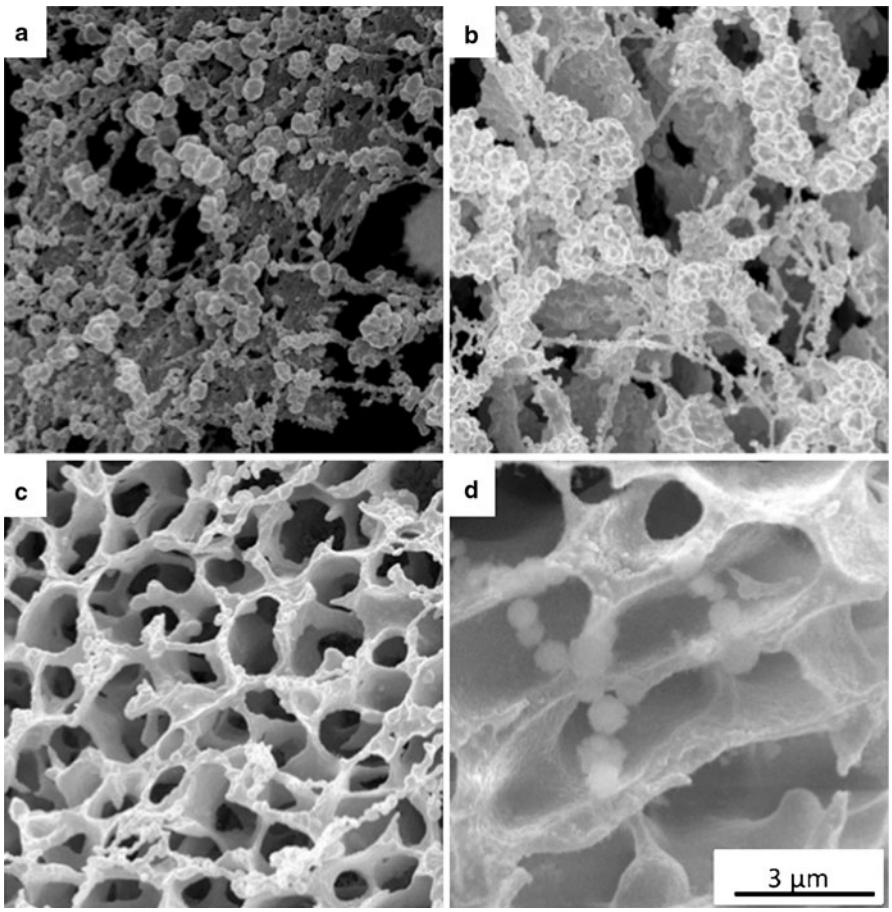

Fig. 6 Cryo-scanning electron micrographs of CaSt SLP containing 10% CaSt and 0.0% (**a**), 1.0% (**b**), 5.0% (**c**) and 10.0% (**d**) P188 processed with three passes through the microfluidizer at 69 MPa followed by crystallization at 22 °C for 24 h

for stabilization of the SLP. It also points to the importance of P188 in achieving a small droplet size during homogenization, rather than preventing SLP aggregation after droplet crystallization.

SLP Stability: Effect of Surfactant Concentration and Storage Temperature

SLP stability is generally considered in terms of the production of small particles (100–200 nm) with a narrow size distribution and the absence of agglomeration and particle growth during storage [7]. Destabilization is common and, in addition to particle size increases, can lead to sample thickening and sometimes gelation. Contributing factors include emulsifier type and concentration, shear, temperature, light and the material of the storage container [19]. In this study, gelation was only observed for the 20 and 30% CaSt systems and never for the 10% lipid samples (Table 1). Preliminary DSC, XRD and SEM experiments suggested gelation was not related to a change in polymorph or morphology (data not shown). Table 4 shows the $D_{4,3}$ and polymorphism for the 10% CaSt SLP (with 0.0, 1.0, or 5.0% P188) stored at 4 and 20 °C for up to 240 days.

An overall effect of time on particle diameter for the 0.0 and 1.0% P188 SLP at both 4 and 20 °C was observed ($P < 0.05$). In contrast, no changes were observed for the 5.0% P188 SLP ($P > 0.05$). The 5.0% P188 samples retained a diameter of ~140 nm at both temperatures, emphasizing the importance of P188 and achieving a narrow size distribution for preventing growth [44]. No changes have been observed either in samples containing 5% CaSt with 5.0% P188 over a period of 6 months (data not shown). Not surprisingly, a trend towards increased particle diameter, related to aggregation and Ostwald ripening, was observed for the 0.0 and 1.0% P188 samples, particularly at 20 °C. The changes in $D_{4,3}$ for the 0.0% P188 samples were relatively modest, although phase separation with particle sedimentation was observed, making representative sampling a challenge. To minimize bias, sampling was done from the midpoint of each 20-mL storage vial.

Less aggregation was observed at 4 versus at 20 °C. Reddy et al. [45] investigated 5% tristearin SLP stabilized with 3% sodium tauroglycocholate, during 30 days storage at 4, 30 and 50 °C and reported size increases at each temperature. Storage at 4 °C was optimal, while samples at

Table 4 Changes in particle diameter ($D_{4,3}$, μm) and polymorphism of P188-CaSt SLP prepared with 10% CaSt and 0.0, 1.0, or 5.0% P188 with a processing pressure of 69 MPa and three passes through the microfluidizer followed by 24 h crystallization at 22 °C (day 0) and storage at 4 and 20 °C for 7, 14, 30, 60, 90, 180 and 240 days

P188 (%)	Time (days)							
	0	7	14	30	60	90	180	240
4 °C								
0.0[a,b]	8.7 ± 0.8 α	15.0 ± 0.5 α	12.7 ± 0.4 α	14.4 ± 0.2 α	36.3 ± 19.7 α	13.6 ± 0.1 α	16.9 ± 1.3 α	23.6 ± 4.8 α
1.0[a]	1.3 ± 0.3 α, β	1.5 ± 0.3 α, β	3.4 ± 0.0 α, β	3.7 ± 0.8 α, β	4.9 ± 0.5 α, β	8.6 ± 3.4 β	9.4 ± 2.3 β	12.6 ± 3.6 β
5.0	0.2 ± 0.0 β	0.1 ± 0.0 β	0.1 ± 0.0 β	0.1 ± 0.0 β	0.1 ± 0.0 β	0.1 ± 0.0 β	0.1 ± 0.0 β	0.1 ± 0.0 β
20 °C								
0.0[a,b]	8.7 ± 0.8 α	21.1 ± 1.1 α	12.7 ± 1.2 α	11.1 ± 0.9 α, β	33.8 ± 1.3 α, β	33.0 ± 3.6 α, β	94.7 ± 12.5 α, β	28.7 ± 1.2 β
1.0[a]	1.3 ± 0.3 α, β	1.5 ± 0.1 α, β	4.2 ± 0.4 α, β	6.7 ± 1.6 α, β	8.4 ± 0.6 β	12.3 ± 6.3 β	11.1 ± 2.2 β	20.4 ± 16.1 β
5.0	0.2 ± 0.0 β	0.1 ± 0.0 β	0.1 ± 0.0 β	0.1 ± 0.0 β	0.1 ± 0.0 β	0.1 ± 0.0 β	0.1 ± 0.0 β	0.1 ± 0.0 β

Values represent means ± SEM, $n = 3$

Assignment of polymorphic form based on spacings of 4.1 Å for α, 4.2 and 3.8 Å for β′, and 4.6 Å for β [15]

Samples for analysis withdrawn from midpoint of 20 mL vial

[a] Indicates significant difference in $D_{4,3}$ observed between days of storage ($P < 0.05$)

[b] Phase separation in progress. Samples from the bottom, midpoint and top of the vial were analyzed periodically by XRD to confirm the presence of only the α polymorph

50 °C experienced the most particle growth, attributed to higher particle kinetic energy promoting collisions and resulting in aggregation [45]. In contrast, Souto et al. [30] reported more extensive growth at low (4 °C) versus high (20 °C) temperatures for tripalmitin SLP stabilized with Tyloxapol (a non-ionic stabilizer) over a 3-month period, although all samples remained in the nanometer range.

In terms of polymorphic changes, only α was observed in the 0.0% P188 SLP throughout storage at 4 °C. At 20 °C, however, these samples began to transition by 30 days and, by day 240, only the β polymorph was present. This is consistent with the greater destabilization observed at 20 versus 4 °C, in terms of $D_{4,3}$ increases. Very similar behavior was observed for the 1.0% P188 samples at 4 and 20 °C. In contrast, the 5.0% P188 SLP existed in the β polymorph from day 0 (the α to β transition initiating around 3 h after production, Fig. 4a). There were no differences for the 5.0% P188 SLP in terms of T_m during the investigated period at either 4 or 20 °C (data not shown, $P > 0.05$) and particle growth was not observed.

The possibility of supercooling and incomplete crystallization was considered in light of the data in Table 4. Melting enthalpies were compared at 4 versus 20 °C and at 0, 7, 30 and 240 days storage for the 5.0% P188 SLP since only the β polymorph was observed (according to DSC, there was a very small α event initially, i.e. $\Delta H_m = 0.1$ J g^{-1}). At day 0, ΔH_m for the β phase (i.e. $\Delta H_{m\beta}$) was 19.4 ± 0.8 J g^{-1}. By day 7, $\Delta H_{m\beta}$ had increased significantly to 26.7 ± 2.6 and 25.9 ± 2.2 J g^{-1} at 4 and 20 °C, respectively ($P > 0.05$). There were no further increases in $\Delta H_{m\beta}$ at days 30 or 240 at either temperature ($P > 0.05$). Therefore, significant increases in the apparent degree of crystallinity were observed for the 5.0% P188 SLP at both 4 and 20 °C within 1 week, although differences between 4 and 20 °C were not observed. The SLP were initially crystallized at 22 °C for 24 h prior to storage at either 4 or 20 °C. The solid fat content (SFC) of the bulk CaSt at 4 and 20 °C was 98.9 ± 0.0 and 99.0 ± 0.1% ($P > 0.05$), respectively, indicating nearly complete crystallization of the lipid droplets at both storage temperatures. Therefore, the degree of supercooling at 4 and 20 °C is expected to be similar. Different behavior was indicated for the 0% P188 SLP where supercooling was not indicated by comparing $\Delta H_{m\alpha}$ of the bulk CaSt versus the dispersed SLP at day 0 (Table 2). Supercooling in the P188-containing SLP is expected based on the decreased droplet size.

In some SLP systems, transitions to the β polymorph have been associated with aggregation, compound expulsion and increased oxidative susceptibility related to increases in surface area [12]. However, there may be opportunities for SLP which exist from very early on in the β polymorph, as long as encapsulation is still permitted. The small diameter, monomodal distribution and absence of aggregation in the 5.0% P188 10% CaSt SLP are all promising factors. Further research is required to determine if encapsulation within the densely packed β polymorph crystalline lattice is possible and, in general, to relate compositional effects with particle properties and encapsulation and release potential to enable the widespread use of SLP.

Acknowledgments The technical assistance of Sandy Smith for the electron microscopy and Sarah Langmaid are gratefully acknowledged. This research was supported by the Natural Sciences and Engineering Research Council of Canada, the Canada Foundation for Innovation, and the Ontario Ministry of Research and Innovation.

References

1. Mehnert W, Mäder K (2001) Solid lipid nanoparticles: production, characterization and applications. Adv Drug Deliv Rev 47:165–196
2. Müller RH, Mäder K, Gohla S (2000) Solid Lipid Nanoparticles (SLN) for controlled drug delivery-a review of the state of the art. Eur J Pharm Biopharm 50:161–177
3. Wissing SA, Kayser O, Müller RH (2004) Solid lipid nanoparticles for parenteral drug delivery. Adv Drug Deliv Rev 56:1257–1272
4. Bunjes H, Unruh T (2007) Characterization of lipid nanoparticles by differential scanning calorimetry, X-ray and neutron scattering. Adv Drug Deliv Rev 59:379–402
5. Westesen K, Drechsler M, Bunjes H (2001) Colloidal dispersions based on solid lipids. In: Dickinson E, Miller R (eds) Food colloids: fundamentals of formulation. Royal Society of Chemistry, Cambridge, pp 103–115
6. Bunjes H, Westesen K, Koch M (1996) Crystallization tendency and polymorphic transitions in triglyceride nanoparticles. Int J Pharm 129:159–173
7. Jenning V, Gohla S (2000) Comparison of wax and glyceride solid lipid nanoparticles (SLN). Int J Pharm 196:219–222
8. Westesen K, Bunjes H, Koch MHJ (1997) Physicochemical characterization of lipid nanoparticles and evaluation of their drug loading capacity and sustained release potential. J Control Release 4:223–236
9. Siekmann B, Westesen K (1994) Melt-homogenized solid lipid nanoparticles stabilized by the nonionic surfactant tyloxapol. I. Preparation and particle size determination. Pharm Pharmacol Lett 3:194–197
10. Müller RH, Mehnert W, Lucks J, Schwarz C, zur Mühlen A, Weyhers H, Freitas C (1995) Solid lipid nanoparticles (SLN)—an alternative colloidal carrier system for controlled drug delivery. Eur J Pharm Biopharm 41:62–69
11. Helgason T, Awad TS, Kristbergsson K, McClements DJ, Weiss J (2008) Influence of polymorphic transformations on gelation of tripalmitin solid lipid nanoparticle suspensions. J Am Oil Chem Soc 85:501–511
12. Weiss J, Decker EA, McClements DJ, Kristbergsson K, Helgason T, Awad T (2008) Solid lipid nanoparticles as delivery systems for bioactive food components. Food Biophys 3:146–154
13. Schwarz C, Mehnert W, Müller RH (1994) Solid lipid particles (SLN) for controlled drug delivery. I. Production, characterization and sterilization. J Control Release 30:83–96
14. Ahmadi L, Wright AJ, Marangoni AG (2008) Chemical and enzymatic interesterification of tristearin/triolein-rich blends: chemical composition, solid fat content and thermal properties. Eur J Lipid Sci Technol 110:1014–1024
15. Chapman D (1962) The polymorphism of glycerides. Chem Rev 62:433–456
16. McClements DJ (2007) Critical review of techniques and methodologies for characterization of emulsion stability. Crit Rev Food Sci Nutr 47:611–649
17. Ghebeh H, Handa-Corrigan A, Butler M (1998) Development of an assay for the measurement of the surfactant Pluronic F-68 in mammalian cell culture medium. Anal Biochem 262:39–44
18. Manjunath K, Reddy JS, Venkateswarlu V (2005) Solid lipid nanoparticles as drug delivery systems. Methods Find Exp Clin Pharmacol 27(2):127–144
19. Freitas C, Müller RH (1998) Effect of light and temperature on zeta potential and physical stability in solid lipid nanoparticle (SLN^{TM}) dispersions. Int J Pharm 168:221–229
20. Bock T, Kleinebudde P, Müller BW (1993) Manufacture of emulsions by means of high pressure homogenization: influence of homogenization parameters, oils and surfactants. In: Benita S, Müller RH (eds) Emulsions and nanosuspensions for the formulation of poorly soluble drugs. Medpharm Scientific Publishers, Stuttgart, pp 201–236
21. Jafari SM, He Y, Bhandari B (2007) Production of sub-micron emulsions by ultrasound and microfluidization techniques. J Food Eng 82:478–488
22. Alexandris P, Hatton TA (1995) Poly (ethylene oxide)–poly (propylene oxide)–poly (ethylene oxide) block copolymers surfactants in aqueous solutions and at interfaces: thermodynamics, structure, dynamics, and modeling. Colloids Surf A Physicochem Eng Asp 96:1–46
23. Mäder K, Mehnert W (2005) Solid lipid particles–concepts, procedures, and physiochemical aspects. In: Nastruzzi C (ed) Lipospheres in drug targets and delivery. CRC Press, New York, pp 1–22
24. Walstra P (1993) Principles of emulsion formation. Chem Eng Sci 48(2):333–349
25. Ahlin P, Kristl J, Smid-korbar J (1998) Optimization of procedure parameters and physical stability of solid lipid nanoparticles in dispersions. Acta Pharm 48:259–267
26. Bunjes H, Koch M, Westesen K (2000) Effect of particle size on colloidal solid triglycerides. Langmuir 16:5234–5241
27. Bunjes H, Steiniger F, Richter W (2007) Visualizing the structure of triglyceride nanoparticles in different crystal modifications. Langmuir 23:4005–4011
28. Freitas C, Müller RH (1999) Stability determination of solid lipid nanoparticles (SLN) in aqueous dispersion after addition of electrolyte. J Microencapsul 16:59–71
29. Saupe A, Gordon K, Radesa T (2006) Structural investigations on nanoemulsions, solid lipid nanoparticles and nanostructured lipid carriers by cryo-field emission scanning electron microscopy and Raman spectroscopy. Int J Pharm 314:56–62
30. Souto EB, Wissing SA, Barbosa CM, Müller RH (2004) Development of a controlled release formulation based on SLN and NLC for topical clotrimazole delivery. Int J Pharm 278:71–77
31. Westesen K, Siekmann B, Koch MHJ (1993) Investigations on the physical state of lipid nanoparticles by synchroton radiation X-ray diffraction. Int J Pharm 93:189–199
32. Helgason T, Awad TS, Kristbergsson K, McClements DJ, Weiss J (2009) Effect of surfactant surface coverage on formation of solid lipid nanoparticles (SLN). J Coll Int Sci 334:75–81
33. Oh J, McCurdy AR, Clark S, Swanson BG (2002) Characterization and thermal stability of polymorphic forms and synthesized tristearin. Food Chem Tox 67:2911–2917
34. Siekmann B, Westesen K (1994) Thermoanalysis of the recrystallization process of melt-homogenized glyceride nanoparticles. Colloids Surf B Biointerfaces 3:159–175
35. Garti N (1982) Crystal structure modifications of tristearin by food emulsifiers. J Am Oil Chem Soc 59:181–185
36. Skoda W, Van den Tempel M (1963) Crystallization of emulsified triglycerides. J Colloid Sci 18:568–584
37. Bunjes H, Koch M, Westesen K (2003) Influence of emulsifiers on the crystallization of solid lipid nanoparticles. J Pharm Sci 92:1509–1520
38. Bunjes H (2005) Characterization of solid lipid nano- and microparticles. In: Nastruzzi C (ed) Lipospheres in drug targets and delivery. CRC Press, New York, pp 41–66

39. Ollivon M (1992) Triglycerides. In: Karleskind A (ed) Manuel des Corps Gras. Lavoisier, Paris, pp 469–503
40. McClements DJ (1999) Emulsion formation. In: Food emulsions. Principles, practice and techniques. CRC Press, Boca Raton, pp 161–184
41. Dingler A, Blum RP, Niehus H, Gohla S, Müller RH (1999) Solid lipid nanoparticles (SLNTM, LipopearlsTM)—a pharmaceutical and cosmetic carrier for the application of Vitamin E in dermal products. J Microencapsul 16:751–767
42. Müller RH, Radtke M, Wissing SA (2002) Nanostructured lipid matrices for improved microencapsulation of drugs. Int J Pharm 242:121–128
43. Ma G, Song C (2006) PCL/Poloxamer 188 blend microsphere for paclitaxel delivery: influence of poloxamer 188 on morphology and drug release. J Appl Polym Sci 104:1985–1999
44. Radke L, Voorhes PW (2002) Coarsening–Basics and growth laws. In: Radke L, Voorhes PW (eds) Growth and coursing. Ostwald ripening in material processing. Springer, New York, pp 117–126
45. Reddy LH, Vivek K, Bakshi N, Murthy RSR (2006) Tamoxifen citrate loaded solid lipid nanoparticles (SLN^{TM}): preparation, characterization, in vitro drug release, and pharmacokinetic evaluation. Pharm Dev Tech 11:167–177